Journal of the Brazilian Society of Mechanical Sciences and Engineering (2018) 40:291
https://doi.org/10.1007/s40430-018-1213-6

TECHNICAL PAPER

# Optimization of processing parameters of cooling slope process for semi-solid casting of ADC 12 Al alloy

Sujeet Kumar Gautam[1,4] · Nilrudra Mandal[2] · Himadri Roy[3] · Aditya Kumar Lohar[1] · Sudip Kumar Samanta[1] · Goutam Sutradhar[4]

Received: 2 February 2018 / Accepted: 26 April 2018 / Published online: 11 May 2018


**Abstract**
In the present work, the effect of processing parameters of cooling slope techniques (pouring temperature, slope angle and slope length) of ADC 12 Al alloy on its microstructural evolution has been studied in detail. A series of cooling slope casting experiments were conducted by varying the pouring temperature (580, 585 and 590 °C), slope length (400, 500 and 600 mm) and slope angle (30°, 45° and 60°). The effect of processing parameters on the response factors, viz. degree of sphericity and particle size, has been investigated by applying analysis of variance (ANOVA), interaction graphs obtained using response surface methodology. The obtained results infer that optimum values of the degree of sphericity (0.865) and particle size (49.30) are observed for the following set of processing parameters, namely 585 °C pouring temperature, 500 mm slope length and 45° slope angle. ANOVA results show that the pouring temperature is the most significant input variables that influence degree of sphericity and particle size followed by slope length and slope angle. The values of output variables obtained from confirmation experiment, performed at 95% confidence level, ensure that they are well within the permissible limits.

**Keywords** Semi-solid processing · Cooling slope process · Response surface methodology · ANOVA

## 1 Introduction

Over the past few decades, a considerable amount of work has been carried out in the field of semi-solid metal processing (SSMP) for its unique competence to form near-net shape products [1, 2]. The key feature in semi-solid metal processing is to generate non-dendritic microstructure under semi-solid condition, in which primary phase of alloy becomes fine and globular in shape throughout the liquid matrix. Compared with conventional techniques, SSMP provides numerous advantages like superior product quality, lower superheat temperature, higher production rate and improvement in mechanical properties through microstructural refinement [3–5]. Rheocasting is an extremely promising SSMP route based on the shear thinning behaviour of alloys with non-dendritic microstructure in the semi-solid state. Rheocasting involves preparation of SSM slurry directly from the liquid melt, followed by a forming process such as pressure die casting (PDC). With "Rheo" processes, the melt is cooled into a semi-solid condition and then is introduced into a mould without the existence of an intermediate solidification step; semi-solid slurry with non-dendritic solid particles (primarily globular is shape) is produced from a completely liquid melt. It is cooled to obtain the desired solid fraction and then it is cast into a component. Component shaping directly from SSM slurries is inherently attractive due to its characteristics, such as overall efficiency in production and energy management.

Technical Editor: Márcio Bacci da Silva.

✉ Sujeet Kumar Gautam
sujeetkumargautam@gmail.com

[1] Advanced Manufacturing Centre, CSIR-Central Mechanical Engineering Research Institute, Durgapur 713209, India

[2] Centre for Advanced Materials Processing, CSIR-Central Mechanical Engineering Research Institute, Durgapur 713209, India

[3] NDT and Metallurgy Group, CSIR-Central Mechanical Engineering Research Institute, Durgapur 713209, India

[4] Department of Mechanical Engineering, Jadavpur University, Calcutta, West Bengal 700032, India

The success of the rheocasting process depends on the production of the semi-solid slurry having fine globular particles of the solid phase surrounded by a continuous film of liquid. Among all prevalent rheocasting techniques, the most popular is the cooling slope (CS) casting process [6, 7] which is simple, has minimal equipment requirements and which can produce a slurry for semi-solid processing. In this technique, there are several key factors (i.e. slope angle, slope length and pouring temperature) which directly affect the morphology of microstructure and mechanical properties. The complexity in optimizing the process parameters in cooling slope technique has led many researchers to delve into this domain of optimization of cooling slope technique. Few such investigations have been highlighted [8–14].

Among various optimization technique utilized, the design of experiments is recognized as one of the most influential statistical techniques to analyse the process variables which affects the responses. Das et al. [11] investigated the optimization of processing parameter of cooling slope technique using Taguchi method. These authors concluded that slope length had maximum effect on morphology (degree of sphericity) of microstructure compared to the other processing parameters (pouring temperature, slope angle and wall temperature). Deepak Kumar et al. [12] also applied Taguchi method to optimize the process parameter of cooling slope casting process for producing semi-solid billet of A356 alloy and A356–$TiB_2$ in situ composite for thixocasting forming process. Khosravi et al. [13] implemented the D-optimal design of experiment method for optimization of input variables of cooling slope process for semi-solid casting of A356 Al alloy. They correlated the combined effect of these parameters (pouring temperature, slope angle, cooling length and isothermal holding time) on the globularity of primary phase of an alloy. Pouvafar et al. [14] used the design of experiment (Taguchi method) to determine an influential effect of each parameter of cooling slope process on the mechanical properties of semi-solid extruded parts.

However, with the advent of new optimization technique such as response surface methodology (RSM), which facilitates a comprehensive understanding of single parameter along with the interaction of parameters from least number of experiments, the understanding of change in process parameters with the output parameters has become clearer. Additionally, RSM process is extensively used in various fields as an optimization technique. Therefore, this work focused on using optimization techniques using response surface methodology for cooling slope process of ADC 12 Al alloy. Based on the literature review, the most common materials used for SSMP as evidenced in the existing literature are A 356, A 357 and A 380 aluminium alloys. Regardless of this fact, ADC 12 aluminium alloy is being widely used as the material in aluminium die cast industry. ADC 12 aluminium alloy has excellent material properties such as high castability, high fluidity and low shrinkage rate [15, 16]. Few investigators have attempted to modify the cast structure of ADC 12 Al alloy using Gas Induced semi solid technique (GISS), Strain-Induced metal activation (SIMA) and Mechanical-Rotatinal-Barrel (MRB) [17–21]. The primary objective of this work is to incorporate rheocasting process using cooling slope technique for ADC 12 Al alloy and thereby optimization of processing parameters of cooling slope process using the response surface methodology. The response's values (degree of sphericity and particle size) of ADC 12 alloy predicted with optimum settings are then evaluated by means of confirmation experiments to verify the validity of this work.

## 2 Experimental procedures

ADC 12 Al alloy has been used for the present work, and liquids and solidus temperatures of this material are 572 and 520 °C, respectively, as validated through DTA result shown in Fig. 1. Table 1 shows the chemical compositions of ADC 12 Al alloy. In the present work, the cooling slope plate made of stainless steel was used for semi-solid slurry generation. ADC 12 ingot was fed inside silicon carbide crucible within the resistance heating furnace and melted at 750 °C. The melt was degassed and poured into holding furnace, which was set at the desired temperature. The holding furnace was placed at the top of cooling slope experimental setup as shown in Fig. 2.

Thermocouples were placed at different locations of the cooling slope as shown in Fig. 2 to measure the temperature and thereby quantify solid fraction within the melt. Under all processing conditions, it was observed that the temperature drop of the slurry at the exit of cooling slope is nearly 40 °C. The cooling slope experimental process was carried out by varying the pouring temperature, slope angle and slope length. Different pouring temperatures (580, 585 and 590 °C) were selected based on available literatures. Cooling slope plate was adjusted with respect to the horizontal plane at different angles (30°, 45° and 60°) and preheated at the constant temperature of 60 °C by using circulation underneath. Arrangements to change the length of the cooling slope plate were also made. Three different slope lengths were considered for the investigation, namely 400, 500 and 600 mm. Prevention of sticking of liquid melt on the cooling plate was then taken care by boron nitride-coated layer on cooling slope plate. In each case, the temperature was monitored using k-type thermocouples, which were placed at three different locations on the slope

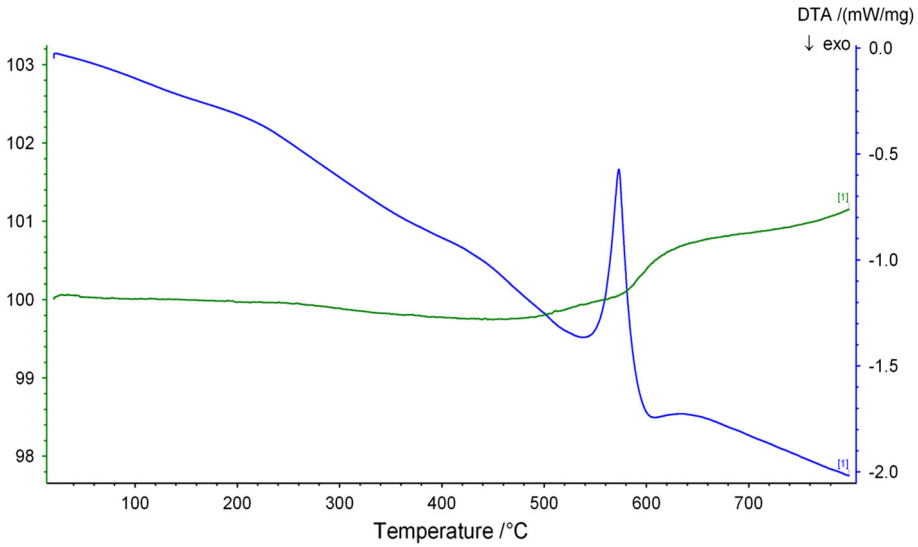


**Fig. 1** DTA curve of ADC 12 aluminium alloy

**Table 1** Chemical composition of ADC12 aluminium alloy

| Element | Si | Cu | fe | Mn | Mg | Zn | Ti | Cr | Ni | Pb | Sn | Al |
|---|---|---|---|---|---|---|---|---|---|---|---|---|
| Mass% | 10.57 | 1.685 | 0.780 | 0.314 | 0.082 | 0.117 | 0.021 | 0.019 | 0.030 | 0.65 | 0.013 | Balance |

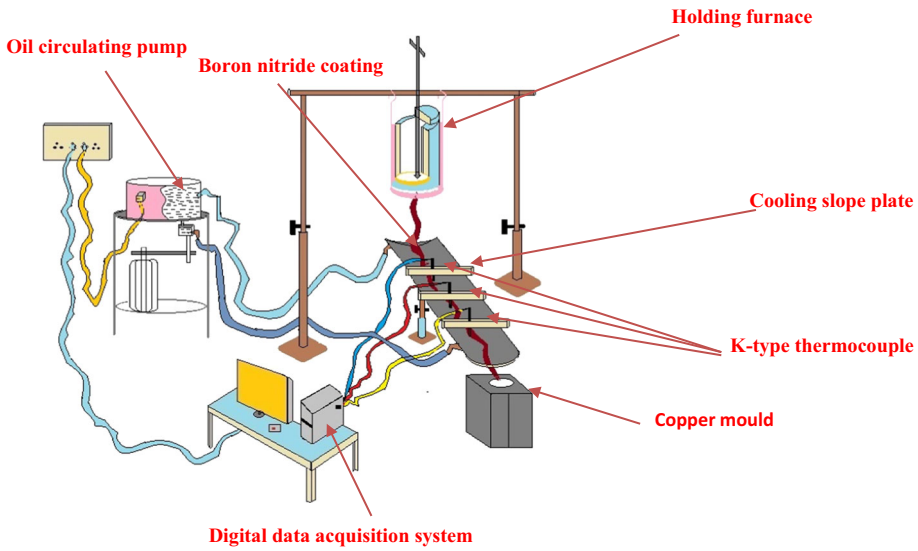


**Fig. 2** Schematic diagram of cooling slope techniques

length and their output was recorded by rapid data acquisition software. At the exit of the cooling slope, the slurry was filled in the preheated copper mould (at 200 °C and then cooled at ambient temperature). The detailed metallographic examination was carried out for both gravity cast material and cooling slope samples, using an optical microscope (M/s Axioimager, Carl Zeiss, UK) and field emission scanning electron microscope (FESEM, Model: ∑igma HD, M/s. Carl Zeiss) for comparative study. The degree of sphericity and particle size for all the samples were quantified from optical images using a commercial image analysis software.

## 3 Systematic plan of investigation

In order of that approach to get a desire aim, the experimental works were planned in the following order:

1. Selection of processing parameters for cooling slope technique.
2. Development of the mathematical model.
3. Checking the adequacy of model by ANOVA method.
4. Confirmation test.

### 3.1 Selection of processing parameters for cooling slope technique

In recent years, many techniques have been developed for the production of semi-solid slurries. One of the most popular SSP techniques is casting using a cooling slope (CS). Cooling slope technique is extensively used for semi-solid slurry generation in semi-solid metal processing, which is accepted by many manufacturing industries. In order to design experimental work, three processing parameters, namely pouring temperature, slope length and slope angle, were chosen as input variables whereas degree of sphericity and particle size obtained from image analysis of each cooling slope rheocast samples were recorded as responses. Material properties of cast component are mainly based on the microstructural characterization of material [22].

Experimental work of cooling slope techniques was studied with response surface methodology (RSM) also known as central composite design. Central composite designs are very useful for sequential experiments, and it efficiently estimates first- and second-order terms. The response surface methodology (RSM) is generally implemented to determine the relationship between the several input variables with responses. A series of trial experiments were carried out to find the limit of input variables. Limits of variables were notified as $-1$, 0 and $+1$ for the lower value, middle value and higher value and also input variables were notified as A for pouring temperature (°C), B for slope length (mm) and C for slope angle (degree). There are 16 test trials performed based on the design on experiment method as shown in Table 2.

The degree of sphericity and particle size were computed using following equations and are tabulated in Table 3.

$$C \cdot D = 2\sqrt{\frac{A_\alpha}{\pi}} \tag{1}$$

**Table 3** Experimental results

| Standard run | Degree of sphericity | Particle size (μm) |
|---|---|---|
| 1 | 0.84 | 50.23 |
| 2 | 0.705 | 69.98 |
| 3 | 0.629 | 82.23 |
| 4 | 0.826 | 52.01 |
| 5 | 0.866 | 49.3 |
| 6 | 0.641 | 75.56 |
| 7 | 0.832 | 54.84 |
| 8 | 0.746 | 68.23 |
| 9 | 0.798 | 62.7 |
| 10 | 0.651 | 72.66 |
| 11 | 0.816 | 56.33 |
| 12 | 0.765 | 65.69 |
| 13 | 0.635 | 76.87 |
| 14 | 0.684 | 71.14 |
| 15 | 0.863 | 49.5 |
| 16 | 0.732 | 67.85 |

**Table 2** Completed design layout

| Run | Standard run no. | Factors | | |
|---|---|---|---|---|
| | | A-pouring temperature (°C) | B-slope length (mm) | C-slope angle (°) |
| 11 | 1 | 585 | 400 | 45 |
| 10 | 2 | 590 | 500 | 45 |
| 4 | 3 | 590 | 600 | 30 |
| 14 | 4 | 585 | 500 | 60 |
| 15 | 5 | 585 | 500 | 45 |
| 2 | 6 | 590 | 400 | 30 |
| 12 | 7 | 585 | 600 | 45 |
| 1 | 8 | 580 | 400 | 30 |
| 9 | 9 | 580 | 500 | 45 |
| 6 | 10 | 590 | 400 | 60 |
| 13 | 11 | 585 | 500 | 30 |
| 5 | 12 | 580 | 400 | 60 |
| 8 | 13 | 590 | 600 | 60 |
| 3 | 14 | 580 | 600 | 30 |
| 16 | 15 | 585 | 500 | 45 |
| 7 | 16 | 580 | 600 | 60 |

$$\text{S.F} = \left(\frac{4\pi A_\alpha}{P_\alpha^2}\right) \tag{2}$$

where $C{\cdot}D$, $A_\alpha$, S.F and $P_\alpha$ show average circular diameter, area, shape factor and perimeter of the primary phase of Al alloy, respectively.

### 3.2 Development of mathematical model

The function of responses and the process parameters can be expressed as

$$Y = f(A, B \,\&\, C) \tag{3}$$

where $Y$ is representing response values.

The second-order regression equation used to represent the response surface for $N$ factors is given by

$$Y = D_o + \sum_{i=1}^{n} D_i X_i + \sum_{i,j=1}^{n} D_{ij} X_i X_j + \sum_{i=1}^{n} D_{ii} X_i^2 \tag{4}$$

where $D_o$ is free term of equation and $D_1$, $D_2$……$D_n$ are the linear term, $D_{11}$, $D_{22}$……$D_{nn}$ are the second-order term and $D_{12}$, $D_{13}$……$D_{n-1,\ n}$ are the interaction terms.

For three input variables such as slope angle, slope length and pouring temperature, the selected polynomial could be expressed as

$$\begin{aligned} Y = {} & D_o + D_1 A + D_2 B + D_3 C + D_{12} AB + D_{13} AC \\ & + D_{23} BC + D_{11} A^2 + D_{22} B^2 + D_{33} C^2 \end{aligned} \tag{5}$$

The values of the coefficients of the polynomial of Eq. (5) have been calculated by the multiple regression method. The Design Expert software (Version 8.0.1) has been used to calculate the coefficient values.

### 3.3 Checking the adequacy of model by ANOVA method

ANOVA method is used to determine the adequacy and significance of the model, additionally to evaluate the effect of lack of fit on model and significance of individual model coefficient. Selecting stepwise backward elimination method to eliminate the insignificant term from the model and result of ANOVA table for the degree of sphericity and particle size are portrayed in Tables 4 and 5, respectively. ANOVA result from Table 4. The Model F-value of 154.60 implies the model is significant. There is only a 0.01% chance that an F-value of this magnitude could occur due to noise. Main effects of pouring temperature (A), slope length (B) and slope angle (C), second-order effect of pouring temperature, slope length and slope angle are significant model terms. Obtained results show that pouring temperature and second order of pouring temperature are the most significant factor compared with slope length and slope angle terms. The latter terms are in turn related to the degree of sphericity, which directly affects mechanical properties. This result is in agreement with that reported in few earlier work [8, 23]. Other remaining significant terms indicate the main effect of slope angle and slope length, the second order of slope angle and slope length having the secondary contribution to the degree of sphericity. Value of P for the lack of fit is greater than 0.05, so it indicates that this model is still significant. The "$R^2$" value is 0.9927, which is close to 1, and therefore is desirable. The value of "Predicted $R^2$" is 0.9653, which is reasonable agreement with the value of "Adjust $R^2$" 0.9862. Adeq Precision measures the signal-to-noise ratio. A ratio greater than 4 is desirable. Value of Adeq Precision 33.537 indicates an adequate signal.

The same methodology is used to find the result of ANOVA for the response of particle size as shown in Table 5 and brought up in quadratic model. Model values of response have been obtained as 455.92 which indicate that model is significant. Value of P for the lack of fit is greater than 0.05, so it indicates that this model is still significant. The "$R^2$" value is 0.9975, which is close to 1, and therefore is desirable. The value of "Predicted $R^2$" is 0.9890, which is reasonable agreement with the value of "Adjust $R^2$" 0.9953. Adeq Precision measures the signal-to-noise ratio. A ratio greater than 4 is desirable. Value of Adeq Precision 60.542 indicates an adequate signal. The main effect of pouring temperature, slope length and cooling slope angle, the second order of slope angle, pouring temperature and slope length and two level of interaction of pouring temperature and slope length are significant model terms. The obtained result is shown in Table 5; pouring temperature and second order of pouring temperature are the most effective significant factor related to particle size. It is easily described by obtained results; pouring temperature condition gives the minimum particle size. It may due to the fact that pouring temperature has the greatest influence on the morphology of microstructure of semi-solid metal casting alloy. The finer size of the primary phase of Al alloy and their higher globularity play a leading role in mechanical properties. The same phenomenon has been reported by Burapa et al. [23]. Mechanical properties are directly proportional to the morphology of microstructure. Furthermore, other remaining significant model terms show the secondary contribution to particle size.

The following equations are the final empirical models in terms of coded factors for:

Degree of sphericity, DOS:

$$\begin{aligned} \text{DOS} = {} & 0.86 - 0.046 \times A - 0.013 \times B + 9.300E \\ & - 003 \times C + 8.375E - 003 \times AB \\ & - 0.11 \times A^2 - 0.026 \times B^2 - 0.041 \times C^2 \end{aligned} \tag{6}$$

Particle size, P:

**Table 4** Final ANOVA for degree of sphericity

| Source | Sum of squares | *df* | Mean square | *F*-value | *p* value prob> | Remarks |
|---|---|---|---|---|---|---|
| Model | 0.11 | 7 | 0.016 | 154.60 | < 0.0001 | Significant |
| *A*-pouring temperature | 0.022 | 1 | 0.022 | 213.52 | < 0.0001 | Significant |
| *B*-slope length | 1.716E−003 | 1 | 1.716E−003 | 17.02 | 0.0033 | Significant |
| *C*-slope angle | 8.649E−004 | 1 | 8.649E−004 | 8.58 | 0.0190 | Significant |
| *AB* | 5.611E−004 | 1 | 5.611E−004 | 5.56 | 0.0460 | Significant |
| $A^2$ | 0.032 | 1 | 0.032 | 319.64 | < 0.0001 | Significant |
| $B^2$ | 1.792E−003 | 1 | 1.792E−003 | 17.77 | 0.0029 | Significant |
| $C^2$ | 4.447E−003 | 1 | 4.447E−003 | 44.10 | 0.0002 | Significant |
| Residual | 8.067E−004 | 8 | 1.008E−004 | | | |
| Lack of fit | 8.022E−004 | 7 | 1.146E−004 | 25.47 | 0.1515 | Not significant |
| Pure error | 4.500E−006 | 1 | 4.500E−006 | | | |
| SD | 0.010 | | *R*-squared | 0.9927 | | |
| Mean | 0.75 | | Adj *R*-squared | 0.9862 | | |
| C.V. % | 1.34 | | Pred *R*-squared | 0.9653 | | |
| Press | 3.816E−003 | | Adeq precision | 33.537 | | |

**Table 5** Final ANOVA for particle size

| Source | Sum of squares | *df* | Mean square | *F*-value | *p* value prob > *F* | Remarks |
|---|---|---|---|---|---|---|
| Model | 1728.64 | 7 | 246.95 | 455.92 | < 0.0001 | Significant |
| *A*-pouring temperature | 173.81 | 1 | 173.81 | 320.88 | < 0.0001 | Significant |
| *B*-slope length | 42.27 | 1 | 42.27 | 78.04 | < 0.0001 | Significant |
| *C*-slope angle | 33.89 | 1 | 33.89 | 62.57 | < 0.0001 | Significant |
| *AB* | 4.22 | 1 | 4.22 | 7.79 | 0.0235 | Significant |
| $A^2$ | 694.44 | 1 | 694.44 | 1282.08 | < 0.0001 | Significant |
| $B^2$ | 15.50 | 1 | 15.50 | 28.62 | 0.0007 | Significant |
| $C^2$ | 43.45 | 1 | 43.45 | 80.22 | < 0.0001 | Significant |
| Residual | 4.33 | 8 | 0.54 | | | |
| Lack of fit | 4.31 | 7 | 0.62 | 30.81 | 0.1379 | Not significant |
| Pure error | 0.020 | 1 | 0.020 | | | |
| Cor total | 1732.97 | 15 | | | | |
| SD | 0.74 | *R*-squared | 0.9975 | | | |
| Mean | 64.07 | Adj *R*-squared | 0.9953 | | | |
| C.V. % | 1.15 | Pred *R*-squared | 0.9890 | | | |
| Press | 19.14 | Adeq precision | 60.542 | | | |

$$P = 49.87 + 4.17 \times A + 2.06 \times B - 1.84 \times C + 0.73 \times AB + 16.23 \times A^2 + 2.42 \times B^2 + 4.06 \times C^2 \quad (7)$$

While, the following equations are final empirical models in terms of actual factors for:

Degree of sphericity, DOS:

$$\begin{aligned}\text{DOS} = {} & -1503.37126 + 5.15697 \times \text{Pouring temperature} \\ & - 7.32285E - 003 \times \text{Slope length} \\ & + 0.017048 \times \text{Slope angle} + 1.67500E - 005 \\ & \times \text{Pouring temperature} \times \text{Slope length} \\ & -4.42276E - 003 \times \text{Pouring temperature}^2 \\ & - 2.60690E - 006 \times \text{Slope length}^2 \\ & -1.82529E - 004 \times \text{Slope angle}^2 \end{aligned} \quad (8)$$

Particle size, P:

$$\begin{aligned} P = {} & 2.22249E + 005 - 759.44838 \times \text{Pouring temperature} \\ & - 1.07164 \times \text{Slope length} - 1.74666 \times \text{Slope angle} \\ & + 1.45250E - 003 \times \text{Pouring temperature} \\ & \times \text{Slope length} \ + 0.64919 \times \text{Pouring temperature}^2 \\ & + 2.42483E - 004 \\ & \times \text{Slope length}^2 + 0.018044 \times \text{Slope angle}^2 \end{aligned} \quad (9)$$

### 3.4 Confirmation test

In order to verify the adequacy of the model developed, six confirmation runs experiments have been executed as explained in Table 6. The experimental test condition for first three confirmation experiment runs is selected from previous casting condition performed, and remaining three experiment runs condition range is chosen outside that operating condition has not been used in previous experiments. Using the prediction capability of design expert software, the degree of sphericity and particle size of selected experiments result are predicted with 95% confidence level. The actual experimental value and the predicted value of all responses are compared and percentage error and residuals calculated. The predicted values of all responses have been determined from Eqs. (8 and 9). The highest percentage errors for the degree of sphericity and particle size have evaluated 0.852 and 2.80%, respectively. Obtained results infer that the predicting ability of models is very well for this application.

## 4 Results and discussion

The SEM micrographs along with EDX analysis of gravity cast and cooling slope cast samples of ADC 12 aluminium alloy are shown in Fig. 3. The observed microstructures reveal that the grain morphologies of ADC 12 aluminium alloy of gravity cast material have typical dendritic structure, along with elongated and needle-shaped eutectic mixtures (Fig. 3a). SEM micrographs show several eutectic morphology of Si-, Cu-$Al_2$- and Fe-rich ($Al_8SiFe_2$) phases (which are conformed by EDX analyses) between the primary phases of Al grain as shown in Fig. 3a. Earlier investigated results on ADC 12 Al alloy show similar microstructures for cast components [24, 25]. The presence of intermetallic eutectic phase such as $Al_8SiFe_2$ in as-cast structure induces more stress concentration, thereby deteriorating its mechanical properties [26]. This limits usage of ADC 12 alloy in as-cast condition. The SEM micrographs of the cooling slope specimen (as shown in Fig. 3b) reveal the nearly globular shape of a primary phase of aluminium alloy. The change in microstructure into the globular morphology of the primary phase in rheocast samples is due to shear forces acting on the solidifying melt along the cooling slope. When molten alloy flows over the cooling slope, it readily loses its superheat and the temperature drops below liquidus temperature which in turn favours nucleation of the primary phase of Al alloy. These nucleated particles get detached and trapped in the flowing melt which is subsequently collected at the bottom of the cooling slope before they fully grow into dendrites [27, 28].

**Table 6** Confirmation run

| S. no. | Parameters | | | Degree of sphericity (DOS) | | | | Particle size (P) | | | |
|---|---|---|---|---|---|---|---|---|---|---|---|
| | Slope angle | Pouring temperature | Slope length | Actual | Predicted | Residual | Error (%) | Actual | Predicted | Residual | Error (%) |
| 1 | 30 | 580 | 400 | 0.745 | 0.742 | 0.003 | 0.40 | 68.93 | 67.42 | 1.51 | 2.24 |
| 2 | 45 | 590 | 500 | 0.710 | 0.704 | 0.006 | 0.852 | 70.28 | 68.72 | 1.56 | 2.27 |
| 3 | 60 | 580 | 400 | 0.762 | 0.760 | 0.002 | 0.263 | 65.25 | 63.74 | 1.51 | 2.37 |
| 4 | 35 | 580 | 550 | 0.757 | 0.756 | 0.001 | 0.132 | 66.24 | 64.60 | 1.64 | 2.54 |
| 5 | 40 | 583 | 600 | 0.814 | 0.811 | 0.003 | 0.37 | 56.06 | 54.53 | 1.53 | 2.80 |
| 6 | 32 | 587 | 450 | 0.786 | 0.783 | 0.003 | 0.383 | 58.22 | 59.68 | − 1.46 | − 2.50 |

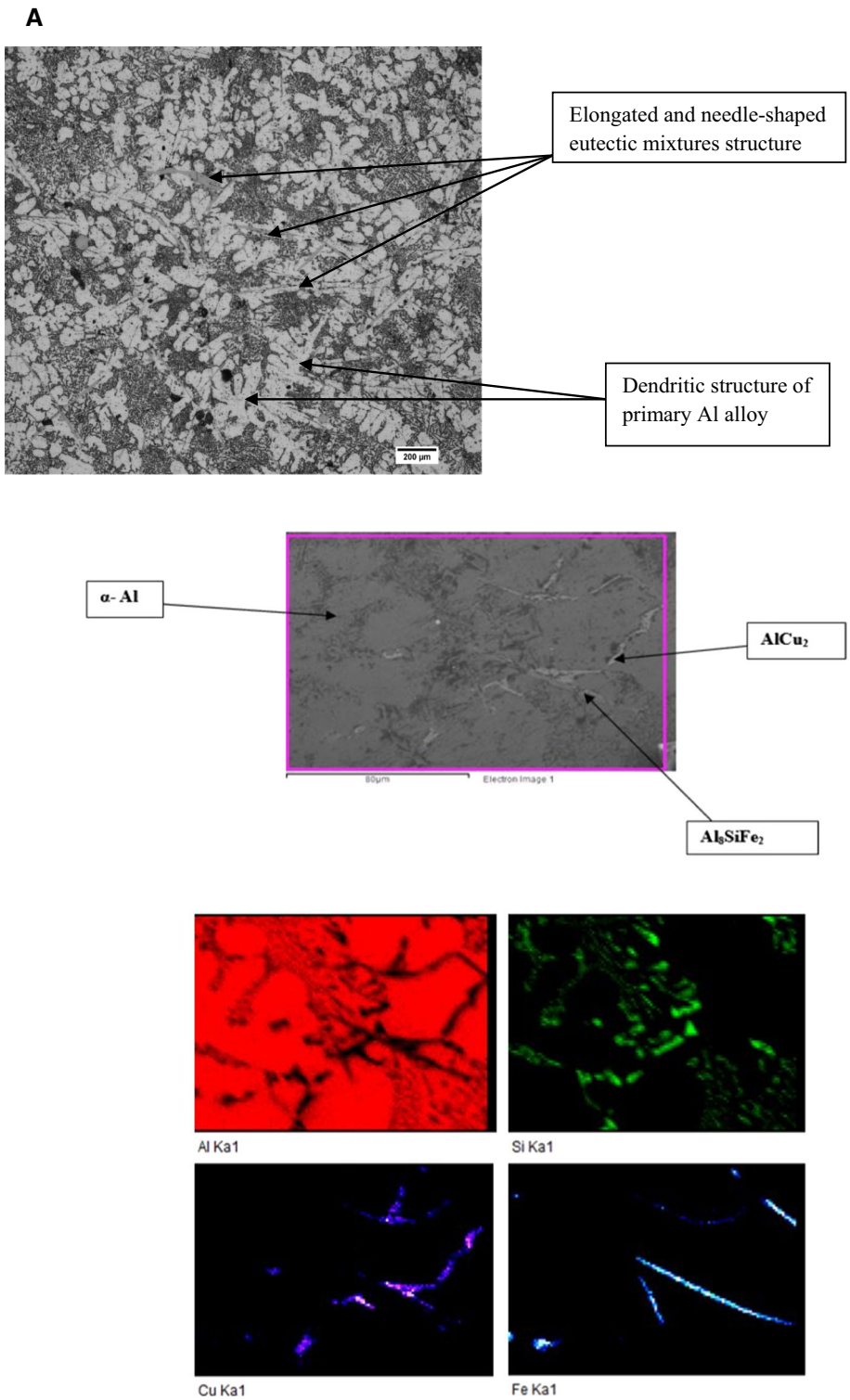


**Fig. 3** **a** SEM micrographs and EDX analyses of the gravity die cast material of ADC12 alloy. **b** SEM micrographs and EDX analyses of the cooling slope cast sample of ADC12 alloy

The microstructure of ADC 12 consists mainly of α-Al phase and eutectic structures based on the amount of Si, Al–Cu and Al–Fe. It is clearly seen from Fig. 3b, the globular primary phase of Al alloy also refines the eutectic phases, which appear as small but well distributed without the needle-like structures.

## 4.1 Direct effect of variables

### 4.1.1 Effect of pouring temperature

Figure 4a–d depicts the microstructures of ADC 12 aluminium alloy at different pouring temperature with

**Fig. 3** continued

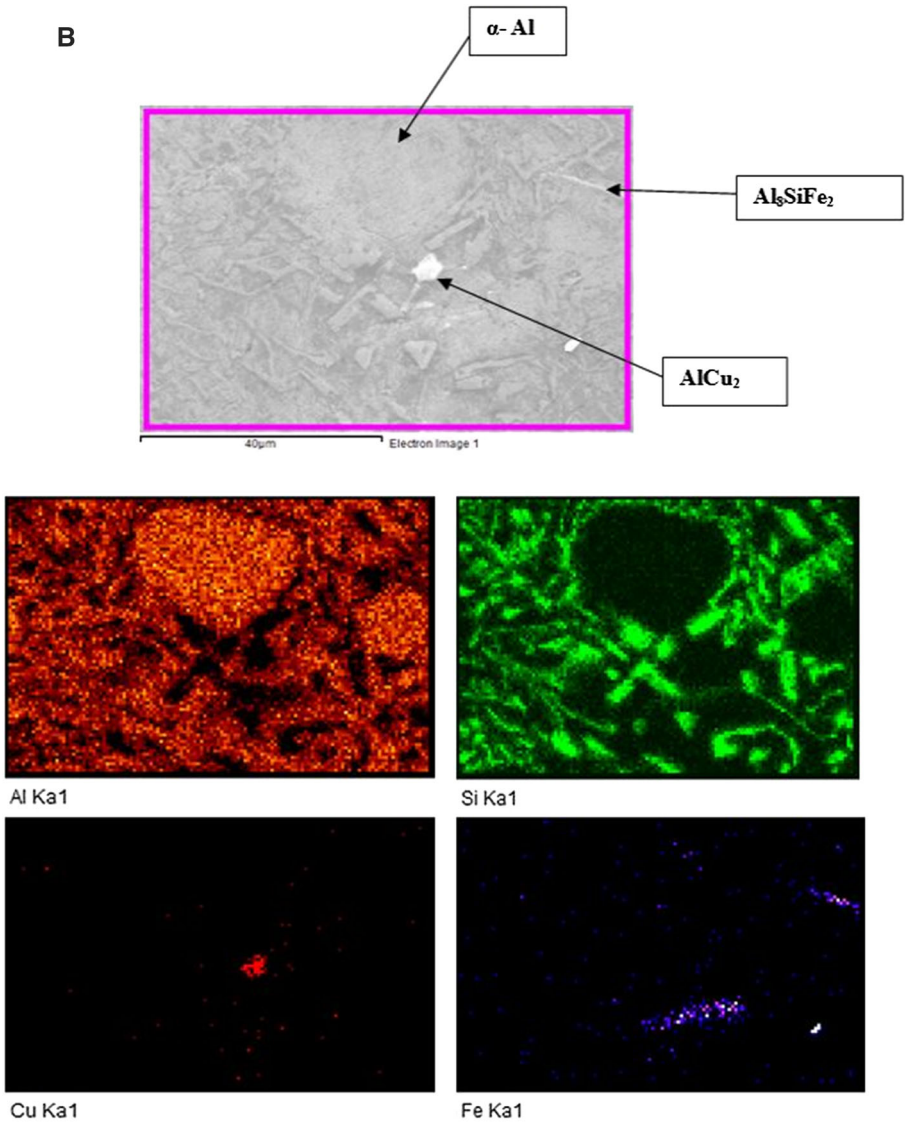


constant slope length and slope angle. The characteristic parameter of cooling slope experiments is listed in Table 2. As shown in Fig. 4a–c, the morphology of primary α-Al grains tends to become globular with decreasing pouring temperature at the end of cooling slope. Figure 4a shows the morphology of primary α-Al grains being irregular and coarser when the pouring temperature is 590 °C. The morphology of the primary α-Al grains changes to spherical at a pouring temperature of 585 °C; however, further decreasing the pouring temperature leads to the loss of sphericity. The same phenomenon has been shown in Fig. 4b, c. The reverse phenomenon is observed for average particles size, i.e. with lowering of pouring temperature the particle size decreases, but beyond 585 °C it again increases. The inflexion point in both these graphs shown in Fig. 4d can be explained from the fact that the initial temperature of the cooling slope is low and it has the chilling effect, which decreases the critical energy of nucleation and critical nuclei radius increases the nucleation ratio. Therefore, a large number of the primary α-Al nuclei will be generated. When pouring temperature is high, the inner wall of cooling slope will be heated, resulting in weakening of chilling effect leading to decrease in nucleation ratio. Moreover, the grains have more time to grow which in turn makes the primary phase coarser [27]. If pouring temperature is lower, the temperature of alloy melt in cooling slope falls rapidly below the liquidus temperature, which helps in nucleation. However, when the pouring temperature is too low, the thickness of solidified shell on cooling slope plate increases markedly, and the chilling effect of cooling slope plate will be weakened further, which inhibits nucleation phenomenon to a great extent [29]. Therefore, from these experiments, it is observed that semi-solid slurry can be prepared

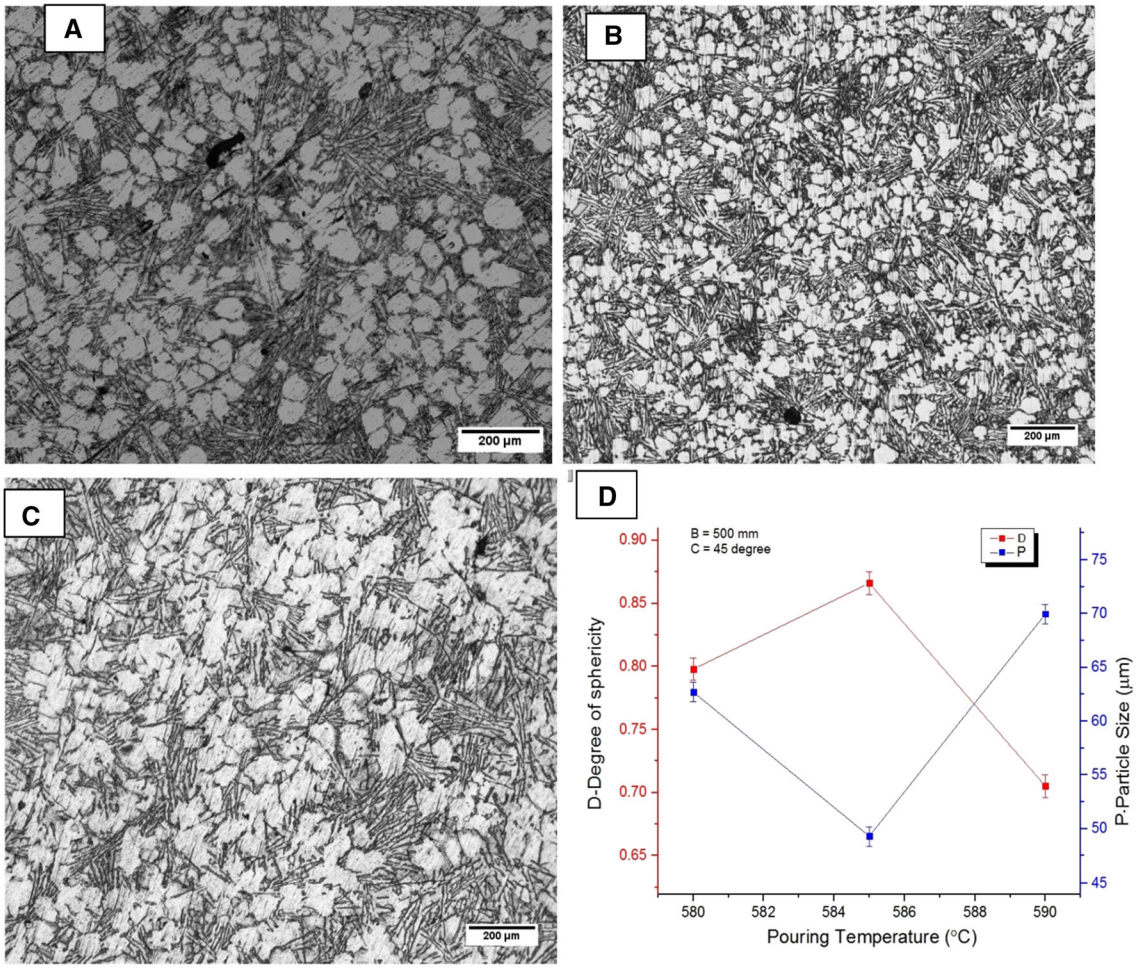


**Fig. 4** Microstructure of rheocast samples at constant slope length (500 mm) and slope angle (45°): **a** 580 °C; **b** 585 °C; **c** 590 °C; and **d** direct effect of processing parameter (pouring temperature)

satisfactorily when the pouring temperature is 585 °C for this class of alloy.

#### 4.1.2 Effect of slope length

Figure 5 shows the variation in the microstructure of rheocast sample at different slope lengths with constant pouring temperature (585 °C) and slope angle (45°). When the slope length increases from 400 to 500 mm, the particle size of primary phase decreases and globularity increases. When the slope length increases from 500 mm to 600 mm, an increase in particle size is observed (Fig. 5d) whereas the sphericity of the particle decreases. This phenomenon can be explained from the fact that with an increase in slope length, the dendritic morphology of cast structure breaks down due to shear forces acting down the cooling slope and the particles form globular in shape, in line with minimization of surface energy. Further, increase in slope length beyond the optimum value (i.e. 500 mm) leads to the higher amount of solid fraction being generated which in turn coarsens the primary α-Al particles [30, 31]. The globularity/sphericity is also decreased.

#### 4.1.3 Effect of slope angle

Slope angle governs flow rate and a contact time between the molten metal and slope surface. Figure 6a shows the change in the particle size and globularity of primary phase of Al alloy due to change of slope angle at constant pouring temperature and slope length. Lower slope angle cannot completely convert the dendritic morphology into globular form of the α-Al phase in the microstructures [26]. Below a certain value of cooling slope angle (i.e. 30° in this case), the molten metal flows slowly and a solid shell forms easily on the cooling slope surface. Increasing the slope angle from 30° to 45° decreases the average size of the primary α-Al grains and increases the globularity as shown in Fig. 6b, c. Increasing the slope angle results in increase in

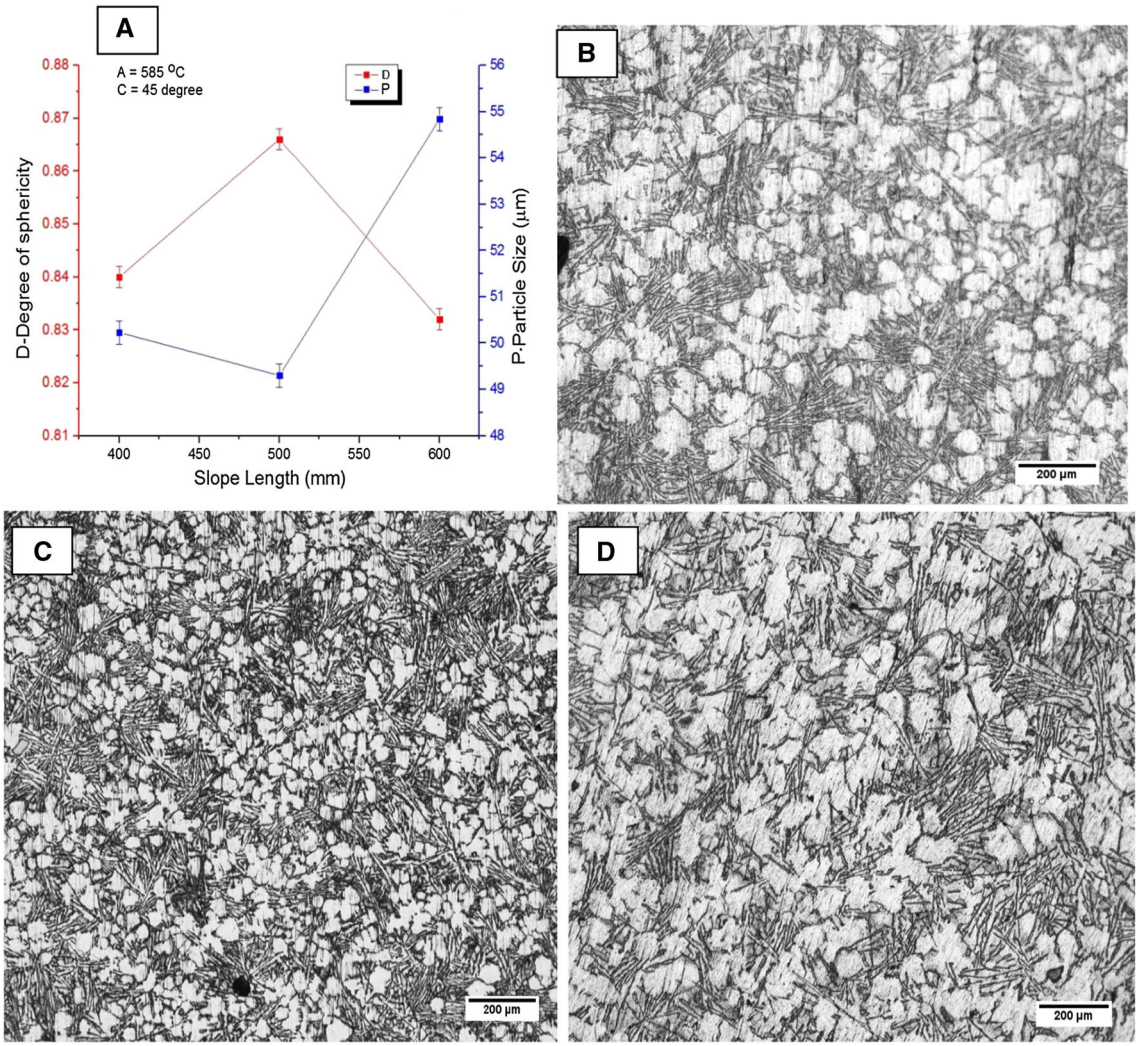


**Fig. 5** Microstructure of rheocast samples at constant pouring temperature (585 °C) and slope angle (45°): **a** direct effect of processing parameter (slope length); **b** 400 mm; **c** 500 mm; and **d** 600 mm

the shear stress that helps to break the dendritic microstructure and converts it to nearly more and more globular and fine grains. When the slope angle is increased further (60°) beyond an optimum value (45° in this case), the slurry passing over the inclined plate travels at a high speed, decreasing the amount of heat dissipated from the molten metal that reaches at the end of the inclined plate. As a result, the collected semi-solid metal contains high liquid fraction and low solid particle in it, which is undesirable [23]. Typical microstructure of samples poured at 60° slope angle is shown in Fig. 6d.

## 4.2 Interaction effect of variables

The interaction effect of pouring temperature and slope length with the degree of sphericity and particle size are shown in Figs. 7 and 8, respectively. Figures 7 and 8 show that globularity increases and particle size decreases with increase in pouring temperature. The relationship between slope length and responses (degree of sphericity and particle size) is almost parabolic. This trend is in good agreement with that of factor effects. High degree of sphericity and lower particle size could be obtained by the optimum pouring temperature at near level 0 of other factors (see Table 2). As seen in Fig. 7, lower pouring temperature negates the formation of primary α-Al phase and increases grain size in the microstructure which thereby causes coarser structure. With increase in the pouring temperature up to an optimum level (585 °C), sufficient formation of primary α-Al phase increases the globularity and decreases the particle size.

However, the further increase in pouring temperature increases particle size and decreases the degree of sphericity [23, 24, 26]. It is also observed from Figs. 7 and

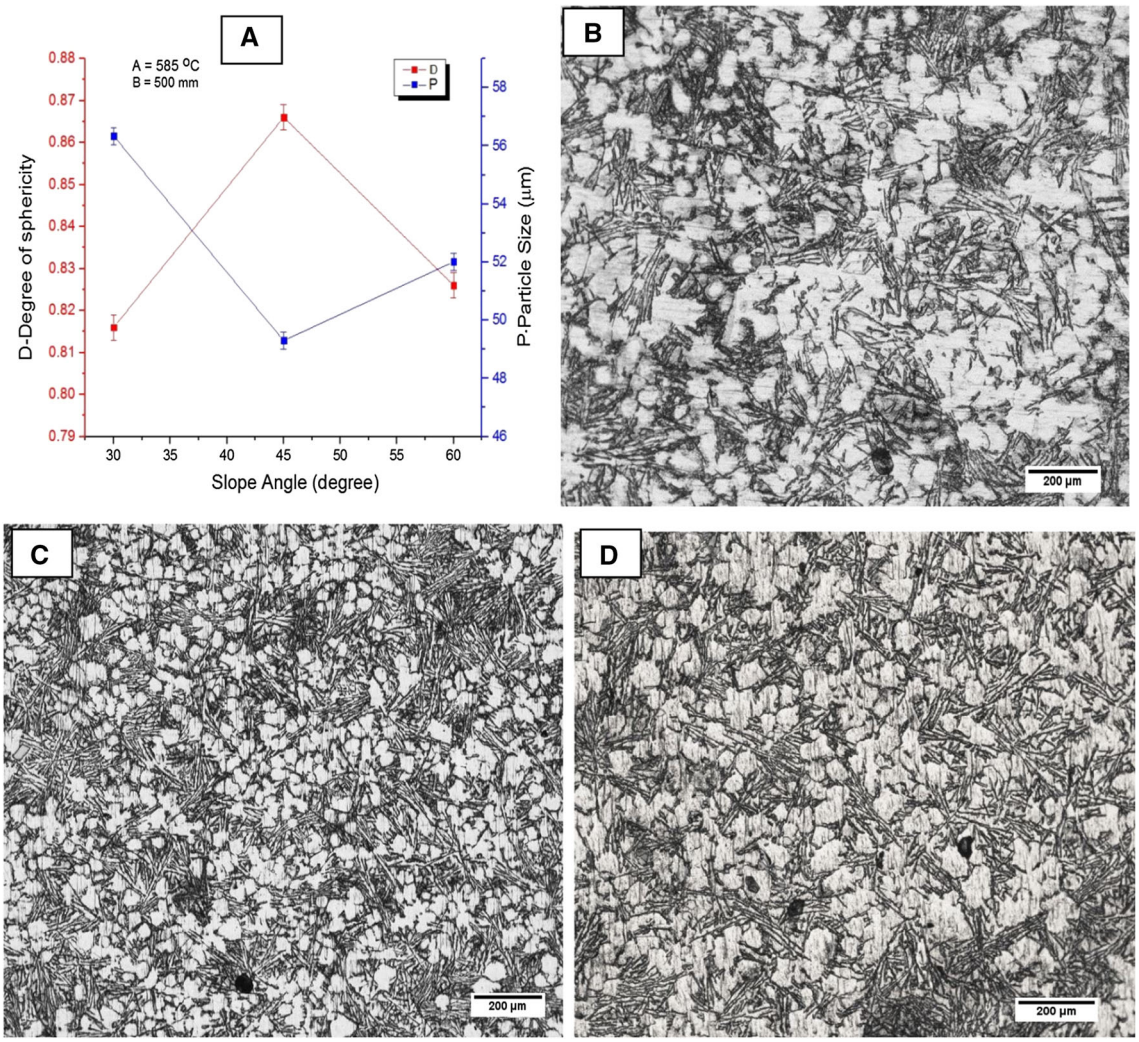


**Fig. 6** Microstructure of rheocast samples at constant pouring temperature (585 °C) and slope length (500 mm): **a** direct effect of (slope angle); **b** 30; **c** 45°; and **d** 60°

8 that increase in slope length noticeably changes the morphology of microstructure. This change is due to the fact that with increase in slope length (400–500 mm) the contact time of the liquid melts increases, thereby enhancing the chances of nucleation of primary α-Al phase and globular microstructure. However, with further increase in slope length (600 mm), the solidification rate on the slope plate increases such that the flow of slurry is unable to detach the solid particles. The solid particles of the slurry adhere to the plate and molten metal does not have contact with the slope and formation of new nucleus does not occur. Increase in the duration time of flow may lead to an increase in the contact and agglomeration of solid particles, which in turn decreases the globularity. This observable fact reveals rosettes and nearly semi-globular in the centre and dendritic character towards the wall zone.

### 4.3 Optimization of parameters

In this experimental study, desirability function optimization of response surface method has been utilized for all responses. During the optimization process, the main objective was to find out the optimal values of processing condition in order to maximize the value of the degree of sphericity and minimize the value of particle size during the casting of ADC12 aluminium alloy using the cooling slope techniques.

The optimal solution for each response is reported in Table 7 with higher desirability level. From Table 7, it can be observed that pouring temperature (585 °C), slope length (500 mm) and slope angle (45°) are optimal processing conditions with 0.937 desirability level for the maximum degree of sphericity and minimum particle size.

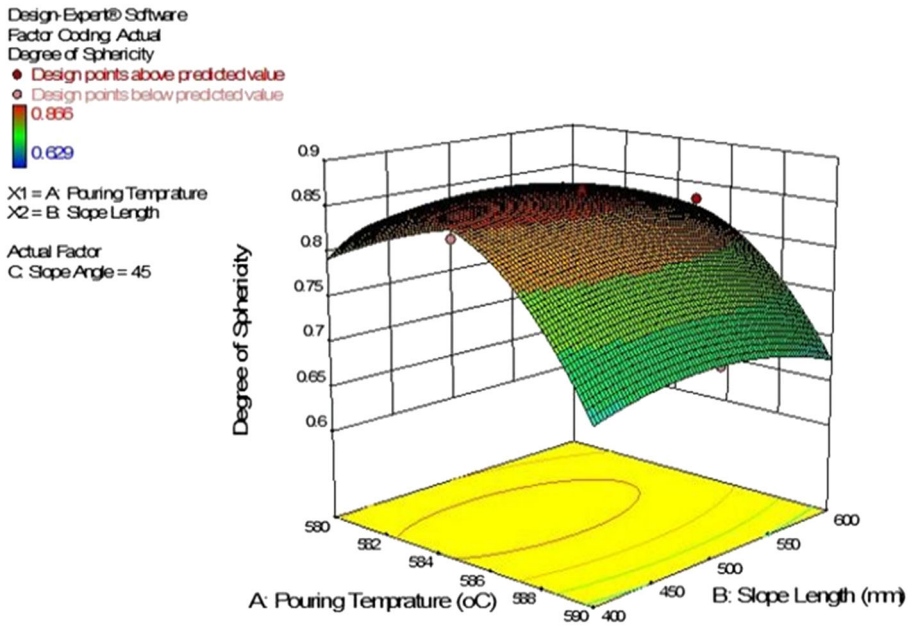


**Fig. 7** 3D surface graph for degree of sphericity

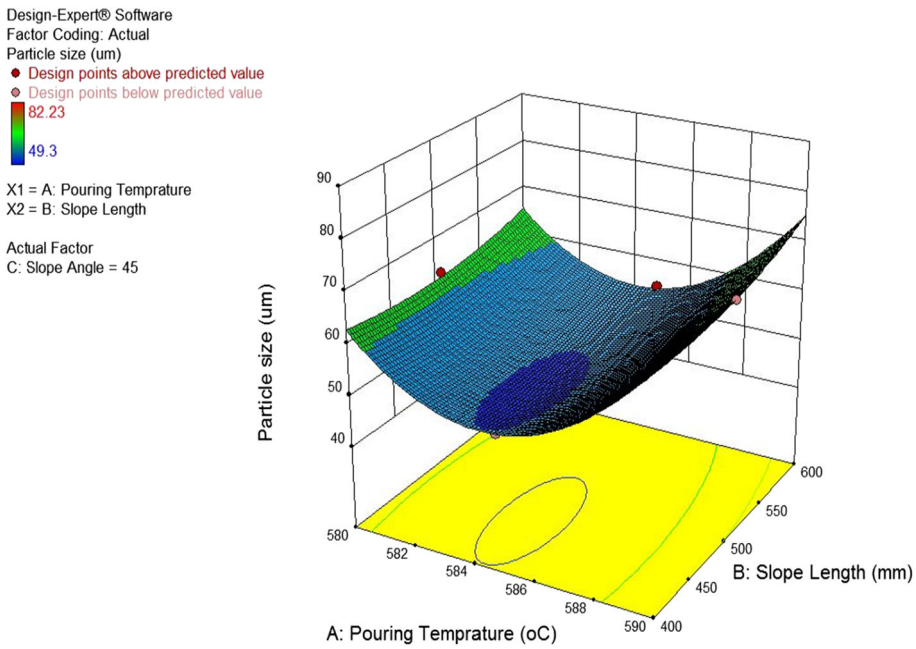


**Fig. 8** 3D surface graph for particle size

**Table 7** Optimization solution

| Number | Pouring temperature | Slope length | Slope angle | Degree of sphericity | Particle size | Desirability | |
|---|---|---|---|---|---|---|---|
| 1 | 585.000 | 500.000 | 45.000 | 0.863 | 49.873 | 0.937 | Selected |
| 2 | 585.000 | 498.340 | 45.000 | 0.863 | 49.840 | 0.935 | |

## 5 Conclusions

The following major inferences are drawn from this investigation:

1. Variation in processing parameters of ADC 12 Al alloy during rheocasting experiments changes the microstructure to a different extent. The optimized properties are obtained during rheocasting with pouring temperature of 585 °C, slope length of 500 mm and slope angle of 45°. These processing conditions result in a maximum degree of sphericity, the value of which is 0.865 and minimum grain size of 49.30 μm of the primary α-Al phase, evaluated experimentally.
2. It is observed that the pouring temperature is the most significant input variables that influence the morphology of microstructure followed by slope length and slope angle, whereas, the interaction effect of input variables (pouring temperature and slope length) also plays a key factor effect in the observed degree of sphericity and particle size.
3. The correlation coefficients of the developed regression models for the degree of sphericity and particle size are 0.9927 and 0.9975, respectively, which confirms the effectiveness of the developed models.
4. The confirmation experiments indicate that the experimental value of responses (degree of sphericity and particle size) of ADC 12 alloy is very close to that of the estimated value from surface response methodology. This confirms the effectiveness of the estimated RSM result which correlated well with that of experimental result, as the error is only 0.852 and 2.80%, respectively.

**Acknowledgements** The authors would like to thank Director, CSIR-Central Mechanical Engineering Research Institute (CMERI) for his kind permission to carry out and publish this work. The authors would like to acknowledge the help rendered by Central Research Facility, CMERI-Durgapur, for material characterization. The authors express their heartfelt gratitude to AdMaC Group (Anmol Khalkho and Anup Rajak) staffs for their support throughout the work.

## References

1. Gencalp S, Saklakoglu N (2010) Semisolid microstructure evolution during cooling slope casting under vibration of A380 aluminum alloy. Mater Manuf Process 25:943–947
2. Taghavi F, Ghassemi A (2009) Study on the effects of the length and angle of inclined plate on the thixotropic microstructure of A356 aluminum alloy. Mater Des 30:1762–1767
3. Spencer DB, Mehrabian R, Flemings MC (1972) Rheological behavior of Sn-15 pct Pb in the crystallization range. Metal Mater Trans B 3:1925–1932
4. Flemings MC (1991) Behavior of metal alloys in the semisolid state. Metal Mater Trans A22:957–981
5. Park C, Kim S, Kwon Y, Lee Y, Lee J (2005) Mechanical and corrosion properties of rheocast and low-pressure cast A356-T6 alloy. Mater Sci Eng A 391:86–94
6. Alhawari KS, Omar MZM, Ghazali J, Salleh MS, Mohammed MN (2017) Microstructural evolution during semisolid processing of Al–Si–Cu alloy with different Mg contents. Trans Nonferr Metal Soc China 27:1483–1497
7. Kaykha M (2017) Effect of angle, length and circulation cooling system on microstructure A360 Aluminum alloy in semi-solid metal forming by cooling slope method. Eng Sol Mech 5:9–14
8. Salleh MS, Omar MZ, Syarif J, Mohammed MN, Allawari KS (2014) Effect of pouring temperature and cooling slope length on microstructure and mechanical properties of rheocast A319 aluminium alloy. Appl Mech Mater 699:251–256
9. Chen YT, Tsao CY, Chiang CH (2014) Making non-dendritic structure via modified cooling slope technique. Adv Mater Res 915:602–607
10. Van Thuong NV, Zuhailawati H, Seman AA, Huy TD, Dhindaw BK (2015) Effects of processing parameters on microstructure evolution of Al–7Si–Mg alloy by cooling slope casting. J Mater Eng Prof 24:2108–2116
11. Das P, Samanta SK, Das R, Dutta P (2014) Optimization of degree of sphericity of primary phase during cooling slope casting of A356 Al alloy: Taguchi method and regression analysis. Measurement 55:605–615
12. Vundavilli PR, Mantry S, Mandal A, Chakraborty M (2014) A Taguchi optimization of cooling slope casting process parameters for production of semi-solid A356 alloy and A356–5TiB2 in situ composite feedstock. Proc Mater Sci 5:232–241
13. Khosravi H, Eslami-Farsani R, Askari-Paykani M (2014) Modeling and optimization of cooling slope process parameters for semi-solid casting of A356 Al alloy. Trans Nonferr Metal Soc China 24:961–968
14. Pouvafar V, Sadough AS, Hosseinj F, Rahmani RM (2010) Design of experiments for determination of influence of different parameters on mechanical properties of semi-solid extruded parts. Trans Nonferr Metal Soc China 20:794–797
15. Tian C, Law J, Van Der Touw J, Murray M, Yao JY, Graham D, Johnd DS (2002) Effect of melt cleanliness on the formation of porosity defects in automotive aluminium high pressure die castings. J Mater Process Technol 122:82–93
16. Zhao HD, Wang F, Li YY, Xia W (2009) Experimental and numerical analysis of gas entrapment defects in plate ADC12 die castings. J Mater Process Technol 209:4537–4542
17. Janudom S, Rattanochaikul T, Burapa R, Wisutmethangoon S, Wannasin J (2010) Feasibility of semi- solid die casting of ADC12 aluminum alloy. Trans Nonferr Metal Soc China 20:1756–1762
18. Wang Z, Ji Z, Hu M, Xu H (2011) Evolution of the semi-solid microstructure of ADC12 alloy in a modified SIMA process. Mater Character 62:925–930
19. Hu ZH, Wu GH, Zhang P, Ding WJ (2013) Rheo-processing of near-eutectic ADC12 alloy. Sol Stat Phenom 192:116–122
20. Hu ZH, Wu GH, Zhang P, Liu WC, Song PANG, Zhang L, Ding WJ (2016) Primary phase evolution of rheo-processed ADC12 aluminum alloy. Trans Nonferr Metal Soc China 26:19–27
21. Hu ZH, Xiang PENG, Wu GH, Cheng DQ, Liu WC, Zhang L, Ding WJ (2016) Microstructure evolution and mechanical properties of rheo-processed ADC12 alloy. Trans Nonferr Metal Soc China 26:3070–3080
22. Kanazawa K, Shibayama K (1997) Effect of heat treatment on fracture toughness and fatigue crack growth characteristics of aluminum alloy die castings. Trans Jpn Socmech Eng 63:478–486
23. Burapa R, Janudom S, Chucheep T, Canyook R, Wannasin J (2010) Effects of primary phase morphology on mechanical

properties of Al–Si–Mg–Fe alloy in semi-solid slurry casting process. Trans Nonferr Metal Soc China 20:s857–s861
24. Chen CL, Thomson RC (2010) Study on thermal expansion of intermetallics in multicomponent Al–Si alloys by high temperature X-ray diffraction. Intermetallics 18:1750–1757
25. Jana S, Mishra RS, Baumann JB, Grant G (2010) Effect of friction stir processing on fatigue behavior of an investment cast Al–7Si–0.6Mg alloy. Acta Mater 58:989–1003
26. Saklakoglu N, Gencalp S, Kasman S, Saklakoglu IE (2011) Formation of globular microstructure in A380 aluminum alloy by cooling slope casting. Adv Mater Res 264:272–277
27. Thaga T, Kapranos P (2002) Simple rheocasting processes. J Mater Proces Technol 130:594–598
28. Birol Y (2007) A357 thixoforming feedstock produced by cooling slope casting. J Mater Proces Technol 186:94–101
29. Chen ZZ, Mao WM, Wu ZC (2011) Influence of serpentine channel pouring process parameters on semi-solid A356 aluminum alloy slurry. Trans Nonferr Metal Soc China 21:985–990
30. Motegi T, Tanabe F, Sugiura E (2002) Continuous casting of semisolid aluminium alloys. Mater Sci Forum 396:203–208
31. Liu W, Tan JB, Li JQ, Ding X (2011) Influence of process parameters by vibrational cooling-shearing slope on microstructures of semi-solid ZAlSi9Mg alloy. Adv Mater Res 211:142–146